







Original Article

EVALUATION OF BONE ADHESIVE BARRIER MEMBRANES FOR GUIDED BONE REGENERATION: AN EXPERIMENTAL STUDY IN RATS

S.E.M. Poos^{1,2,*}, M. van Erk^{1,§}, B.A.J.A. van Oirschot³, S.C.G. Leeuwenburgh³,
R.P. Félix Lanao², H. van Goor¹ and J.J.J.P. van den Beucken³

¹Department of Surgery (route 618), Radboud University Medical Center, 6500 HB Nijmegen, The Netherlands

²GATT Technologies BV, 6534 AT Nijmegen, The Netherlands

³Department of Dentistry-Regenerative Biomaterials, Radboud University Medical Center, 6525 EX Nijmegen, The Netherlands

[§]These authors contributed equally.

Abstract

Background: Guided bone regeneration (GBR) procedures require barrier membrane fixation to ensure membrane and graft stability. Recently, innovative resorbable fibrous gelatine membranes have been developed with a coating based on poly(2-oxazoline) (POx) polymer modified with mineral-adhesive alendronate (POx-Ale) and/or amine-reactive *N*-hydroxysuccinimide groups (POx-OH-NHS) to obtain bone-adhesive properties. We here assessed the *in vivo* tissue adhesive properties and the effect on bone growth and biocompatibility of novel GBR membranes in a non-critical rat cranial defect model. **Methods:** In 60 rats ($n = 12$ per group), experimental bone adhesive GBR membranes (POx-Ale, POx-OH-NHS, and POx-Ale/POx-OH-NHS mixture) and control membranes (non-coated control and collagen Bio-Gide membranes) were evaluated upon application as covers on non-critical cranial defects ($\varnothing 4$ mm). Tissue adherence, bone growth, biocompatibility, membrane degradation and tissue responses were assessed by macro- and microscopic evaluation after 5- and 14-days implantation. **Results:** Membrane adherence to bone tissue upon application was significantly higher for POx-Ale ($p = 0.003$), POx-OH-NHS ($p = 0.000$), POx-Ale/POx-OH-NHS polymer ($p = 0.000$), and non-coated membranes ($p = 0.006$) compared to Bio-Gide membranes, although this effect was no longer visible after 5 and 14 days of implantation. A lower cohesive strength and more fragmentations of the POx-coated membranes were detected in comparison to both control membranes. At these short implantation periods, all membranes showed similar levels of bone regeneration in the cranial bone defect area. Although adverse tissue reactions were not observed for any of the membranes, POx-coated membranes swelled more than Bio-Gide membranes. **Conclusions:** Novel bone adhesive GBR membranes demonstrated improved adherence upon application to bone tissue compared to commercially available Bio-Gide membranes.

Keywords: Poly(2-oxazoline), rat, cranial defect, bone adhesive, barrier membrane, guided bone regeneration.

***Address for correspondence:** S.E.M. Poos, Department of Surgery (route 618), Radboud University Medical Center, 6500 HB Nijmegen, The Netherlands; GATT Technologies BV, 6534 AT Nijmegen, The Netherlands. Email: steven.poos@radboudumc.nl.

Copyright policy: © 2025 The Author(s). Published by Forum Multimedia Publishing, LLC. This article is distributed in accordance with Creative Commons Attribution Licence (<http://creativecommons.org/licenses/by/4.0/>).

Introduction

The amount of bone volume in a dental defect has a significant influence on the initial stability of a dental implant. A strong primary stability upon implant application is essential for a successful osseointegration, the process where interfacial bone is formed to envelop the dental implant [1–3]. The long-term stability of a dental implant is affected by multiple factors, like bone volume, bone quality, and the location and depth of implant placement [4]. Furthermore, resorption of bone tissue at the tooth extraction site is mostly unavoidable after tooth removal, which

can cause up to 50 % bone loss in a year [5,6]. This can result in significant ridge dimensional changes, bone dehiscence, and increased cavities at the tooth extraction site.

Guided bone regeneration is an important technique to prevent bone resorption and promote implant stability, but improvements in membrane fixation and biocompatibility remain urgently needed. Guided bone regeneration is a ridge augmentation technique that uses barrier membranes and bone grafts that enable osteoblast infiltration at the defect surfaces while blocking soft tissue cells that can impede bone formation [7–10]. It is essential that the barrier membranes are fixated to the tissue bed so that it remains

in place during the initial bone formation phase [11–13]. In general, non-degradable membranes are fixated with titanium pins that require removal after full bone regeneration in a second surgical intervention. Resorbable membranes are either fixated with resorbable sutures or placed loosely over the defect with associated risks of membrane dislodgement or -collapse [7,9,11,14,15]. Tissue adhesives are potentially valid alternatives for resorbable membrane fixation but rarely used as current adhesives lack sufficient bonding strength or good biocompatibility [16–18].

Barrier membranes coated with novel bone adhesive polymers based on poly(2-oxazoline)s (POxs) hold promise as a barrier membrane and adhesive fixative in one, thereby overcoming shortcomings of current resorbable barrier membranes [19]. These POxs are conjugated with alendronate, a bisphosphonate with a strong affinity to the mineral content of hydroxyapatite, which enables this polymer (POx-Ale) to adhere to bone tissue [20]. Furthermore, the functionalization of POx with NHS-ester groups (POx-OH-NHS) enables covalent binding to amines in blood, soft and hard tissue, which results in haemostasis and tissue binding [21]. Membrane prototypes have been created by coating a fibrous gelatine membrane with a combination of these polymers and a polyester backing layer to provide sufficient mechanical strength. Initial experiments focused on the adhesive and cohesive strengths of the novel membranes and showed their improved initial adherence (<1 day) in *ex vivo* and *in vivo* pig models [22,23]. However, the membrane's *in vivo* tissue adhesive properties and biocompatibility have not yet been addressed.

In this study we aimed to determine the effect of the novel membranes on bone/tissue adhesive capabilities, bone growth, and short-term biocompatibility in a rat cranial model. A non-critical rat cranial defect was used to assess the membrane's performance in comparison to an industrial standard product on the basis of membrane cohesion, -stability and -adherence to tissue after 5 and 14 days. Furthermore, histological analysis determined the membrane degradation, inflammation rate and the amount of neoformed bone at the defect site after 5 and 14 days.

Methods

Animals

The study was performed at the Central Animal Laboratory of Radboud University according to the Planning Research and Experimental Procedures on Animals (PREPARE) guidelines and reported following the Animal Research: Reporting of *In Vivo* Experiments (ARRIVE) guidelines [24,25]. This study is also in compliance with ISO 10993-6 [26]. Sixty adult male Wistar rats (Hsd-Cpb:WU; Envigo, Horst, the Netherlands) weighting 380 ± 20 g were used. All rats were housed in standard Type III cages (1291H; Techniplast, Buggugiate, Italy) in pairs with food (V1534-000, 919118969; Ssniff, Uden, the Netherlands) and water ad libitum. Cages were enriched with nest-

ing material (14180; Sizzle nest, Plexx, Elst, the Netherlands), a gnawing stick and a retreat. After surgery, the retreat was replaced by an orange plate over the cage to protect the rats from rubbing the fresh wound. A standard 12 hours light/dark cycle and a temperature of 22–23 °C were maintained in the rooms. The animals were randomly assigned to their cages and randomly placed on shelves in the animal room. All rats had a minimum 5-day acclimatization period before surgery. Animals were checked at least twice daily and scored for dehydration, fur, activity, breathing, wounds and cleanliness of the nose and eyes. Prior to the study, humane endpoints were defined: animals were to be sacrificed if they showed signs of severe discomfort (drop in body weight of 20 % or more, compared to starting weight).

Experimental Design

Animals were divided into five groups, depending on the applied membrane. Three experimental membranes, one non-coated control membrane (negative control) and a commercial barrier membrane used as predicate device (500622; Bio-Gide, GeistlichPharma AG, Wolhusen, Switzerland, positive control) were included. In each animal, two bilateral cranial defects were created (Fig. 1) and each was covered with a different membrane. Allocation of the membranes was performed using a block randomization, excluding combinations with two identical membranes in one animal. The pairs of membranes were randomly allocated to an animal using the ASELECT function in Microsoft Excel (Version 2505; Microsoft, Redmond, WA, USA). Surgeons were blinded for membrane type both during the surgical procedure and at sacrifice of the animals. Membranes were implanted for 5 and 14 days to visualize the inflammatory reactions in wound healing and to visualize the beginning of bone regeneration, respectively. All membrane types were tested $n = 12$ per implantation period.

Membranes

Three different experimental membrane types and a negative control membrane were prepared, containing a gelatine base layer consisting of three layers gelatine-based fibrillar Tuft-it® material (GF-7365; 5×7.5 cm, Gelita Medical, Eberbach, Germany) and a polyester backing layer (5×7.5 cm) consisting of poly(lactic-co-glycolic acid) (PLGA, 8 wt %), poly(L-Lactide-co- ϵ -caprolactone) (P(LA-CL), 67 wt %), and amine-functionalized poly(2-oxazoline) (POx-NH₂, 25 wt %) to enhance the mechanical strength of the resulting membranes. To create tissue adhesive characteristics, the gelatine membrane base layer was coated with either POx-Ale (70/30 %), POx-OH-NHS (60/20/20 %) or the 1:1 (w/w) combination of POx-Ale and POx-OH-NHS. Preparation of the POx-polymers for membrane coating was described in detail previously [19,20].

Samples were loaded in the membrane base layer via dry deposition in two cycles (40 kV, 100 Hz, 20 seconds)

Table 1. Outcomes and measures used for the evaluation of the experimental- and control membranes.

Parameter	Scoring		Description
Upon application			
Adhesive strength (membrane)	0	No adherence	Shifting of the membrane over bone defect
	1	Weak adherence	Partial attachment of the membrane
	2	Moderate adherence	Detachment of membrane after pulling the membrane with tweezers
	3	Strong adherence	Attachment of membrane, also after pulling the membrane with tweezers
After sacrifice			
Abscesses (periosteum)	Yes/no		
Redness (periosteum)	0	No redness	
	1	Mild redness	
	2	Moderate redness	
	3	Severe redness	
Covering defect (membrane)	Yes/no		
Detachment (membrane)	Yes/no		
Swelling (membrane)	Yes/no		
Displacement (membrane)	Yes/no		
Tissue encapsulation	Yes/no		
Adhesive strength (membrane)	0	No adherence	Shifting of the membrane over bone defect
	1	Weak adherence	Partial attachment of the membrane
	2	Moderate adherence	Detachment of membrane after pulling the membrane with tweezers
	3	Strong adherence	Attachment of membrane, also after pulling the membrane with tweezers
Cohesive strength (membrane)	0	Low cohesion	Severe fragmentation of the membrane
	1	Medium cohesion	Partial fragmentation of the membrane
	2	High cohesion	No fragmentation of the membrane
Inflammatory cell infiltration	0	0–25 %	Percentage of all cells in defect area
	1	26–50 %	Percentage of all cells in defect area
	2	51–75 %	Percentage of all cells in defect area
	3	76–100 %	Percentage of all cells in defect area
Ehrlich & Hunt scale	0	No evidence	No evidence of inflammatory cells at interface
	1	Occasional evidence	Occasional evidence of inflammatory cells at interface
	2	Light scattering	Light scattering of inflammatory cells at interface
	3	Abundant evidence	Abundant evidence of inflammatory cells at interface
Neoformed bone	4	Confluent cells	Confluent cells or fibres of inflammatory cells at interface
	0	No bone formation	No neoformed bone
	1	Little bone formation	Bony bridging only at defect borders (<50 %)
	2	Mediate bone formation	Bony bridging over partial length of defect (>50 %)
	3	Almost complete bone bridging	Bony bridging entire span
Soft tissue growth	4	Complete bone bridging	Bony bridging entire span and depth defect
	0	No soft tissue growth	No soft tissue growth in defect area
	1	Little soft tissue growth	<50 % soft tissue bridging in defect
	2	Mediate soft tissue growth	>50 % soft tissue bridging in defect area
Membrane degradation	3	Almost completely filled with soft tissue	Complete soft tissue bridging in defect area
	4	Completely filled with soft tissue	Soft tissue bridging entire span and depth defect
	0	No degradation	Membrane (almost) complete and intact
	1	Moderate degradation	Membrane fragmentation with at least one large part
	2	Severe degradation	Membrane fragmentation with all small parts
	3	Complete degradation	No membrane parts visible

Table 2. Overview of sample retrieval after implantation.

Groups	Macroscopic assessment		Histological assessment	
	5 days	14 days	5 days	14 days
a POx-Ale	12	12	11 [‡]	12
b POx-OH-NHS	11*	12	9 [‡]	11 [‡]
c POx-Ale/POx-OH-NHS (1:1)	11*	12	10 [‡]	11
d Non-coated (–control)	12	12	11 [‡]	12
e Bio-Gide (+control)	12	12	11 [‡]	12
Total	60	60	52	58

*Specimen lost due to premature death of animal. [‡]Specimen loss due to technical issues during histological processing. POx, poly(2-oxazoline); Ale, alendronate; OH-NHS, *N*-hydroxysuccinimide.

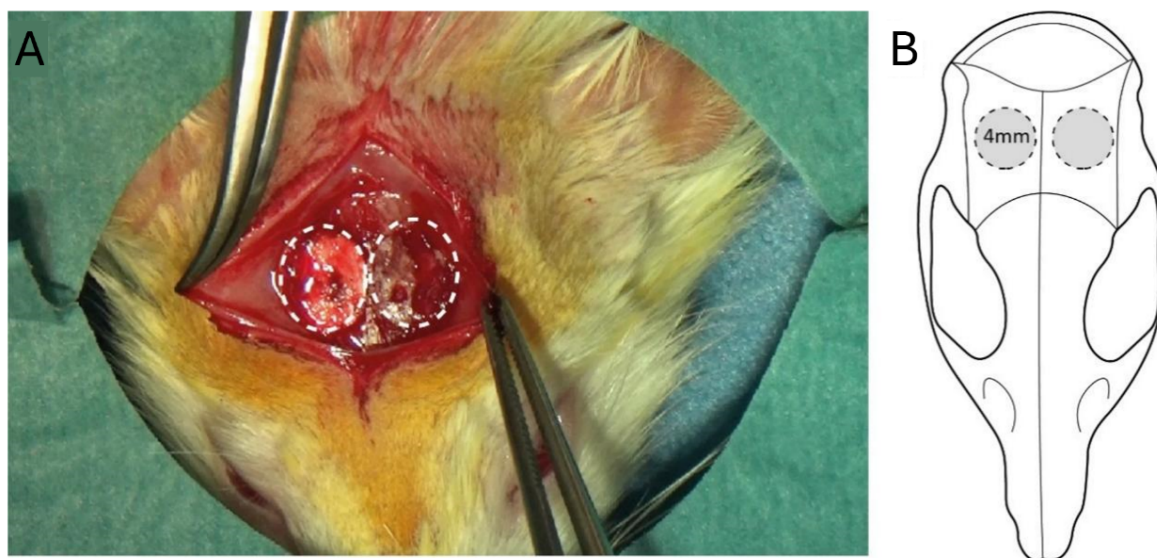


Fig. 1. Defect model overview. (A) Representative intra-operative image of the membranes placed over the filled cranial bone defects. Dashed circles indicate membranes covering bone defects (4 mm diameter). (B) Schematic representation of rat calvarial bone defects (4 mm diameter) created bilaterally.

using a high voltage electrostatic impregnation system (S-Preg; Fibroline, Limonest, France). On the POx-Ale membrane a total of 0.46 g polymer powder was loaded (5×7.5 cm), 0.37 g for the POx-OH-NHS membrane and a total of 0.43 g powder on the membrane containing both POx-Ale and POx-OH-NHS (1:1 ratio) polymer. Two layers of polyester backing were simultaneously adhered to the membrane base layer by pressing two times for three seconds using a heated iron (150 °C, ~ 30 N; DST3031/20; Philips, Amsterdam, the Netherlands). Membranes were cut in individual parts of 8×8 mm and dried overnight at 40 °C in a vacuum oven (201706231301; VWR, Radnor, PA, USA). Thereafter, membranes were individually sealed under vacuum in Alu-Alu pouches (BM00024496-0000; LamiZip, Daklapack Europe, Lelystad, the Netherlands) and sterilized using e-beam in a range from 25–35 kGy (Steris, Mentor, OH, USA).

The negative control membrane consisted of a non-coated control membrane, containing a gelatin base layer and a polyester backing layer, but without any bone ad-

hesive coating. The commercial membrane Bio-Gide consisted of natural porcine collagen I and III [27].

Surgical Procedure

Rats were weighed on the day of surgery and received analgesia (Buprenorphine, Bupaq; 2308229AF; 0.02 mg/kg, Richter Pharma, Wels, Austria) at least 15 minutes before surgery. After anesthetizing the animal (Isoflurane, induction 5 %, maintenance 2.5 % in 1:1 mixture of O₂ and pressurized air), the head was shaved from neck to eyes. The shaven area was cleaned with 70 % ethanol and disinfected with iodine tincture. The rat was then placed on a heat mat with a temperature sensor which maintained the body temperature between 36–38 °C. A pulse oximeter was clamped onto the foot to monitor heart rhythm and oxygenation of the blood, and a temperature sensor was inserted in the anus. A sterile hole towel was placed over the rat. The rats were operated using strict aseptic techniques. The skin was opened with a surgical blade (nr.10) and a few drops from the defect of blood were collected for homoge-

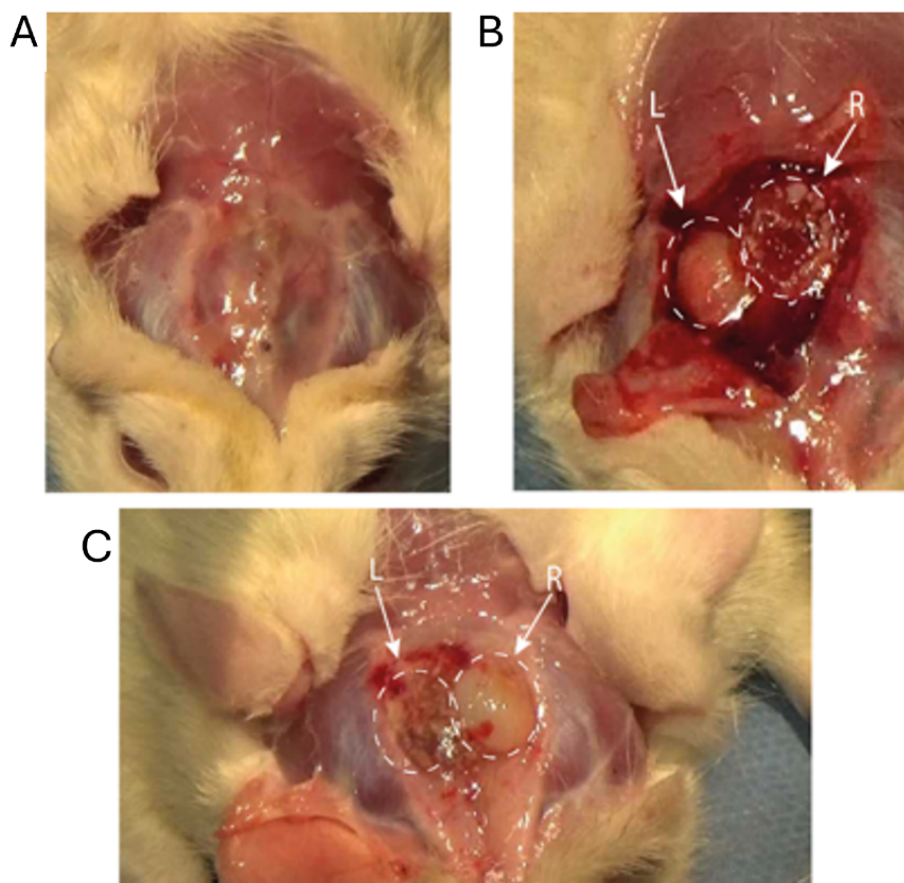


Fig. 2. Skull images after sacrifice. (A) Representative image of closed periosteum after sacrifice. (B) Image of sacrificed rat with opened periosteum with Bio-Gide® membrane (L) and POx-Ale/POx-OH-NHS membrane (R) 5 days after implantation. (C) Representative image of membranes (POx-Ale membrane (L), Bio-Gide® membrane (R)) covered with a fibrous layer 14 days after implantation. POx, poly(2-oxazoline); Ale, alendronate; OH-NHS, *N*-hydroxysuccinimide.

nizing the Bio-Oss® (500606; GeistlichPharma AG, Wolhusen, Switzerland) bone substitute. Local analgesia was applied by a few drops of a mixture (2:1) of Lidocain (10 mg/mL; 18Z3873; Fresenius Kabi, Bad Homburg vor der Höhe, Germany) and bupivacaine (5 mg/mL; 30102A-1; Aurobindo Pharma BV, Hyderabad, India) onto the periosteum. After at least one minute the periosteum was incised and elevated. One defect was drilled in each section of parietal bone (Fig. 1A) using a dental drill (2021-1036215; motor unit: Astratech Elcomed 100, Bürmoos, Austria; hand piece: MASTERmatic LUX M20 L, KaVo, Biberach, Germany), and a trephine burr with outer diameter of 4 mm (229L 030, Hager & Meisinger GmbH, Neuss, Germany) assuring not to damage the dura mater. A mix of Bio-Oss® S particles and autologous blood was used to fill the created bone defects and gently pressed on the bone tissue and graft (Fig. 1B). Adherence of the membrane directly after application was scored by two researchers. Subsequently, the periosteum was closed over the defects with a running suture (Monocryl 6-0, C9260, Ethicon, New Brunswick, NJ,

USA) and the skin was closed with staples. The rats were allowed to recover in an incubator (30 °C, with added oxygen), after which the animals were placed back in their cage. At 12, 24, 36 and 48 hours postoperatively the animals received analgesia (Buprenorphine, Bupaq, 0.02 mg/kg).

At 5 or 14 days the animals were asphyxiated with CO₂ and the skin was carefully reopened. State of the periosteum, surrounding soft tissues and membrane were scored and the skull from occipital bone to frontal bone was excised for histological analyses.

Histological Processing

The skull bones were placed in a 4 % buffered formaldehyde solution for 48 hours and then in a 10 % EDTA solution for decalcification. After two to three weeks, the samples were transferred to 70 % ethanol for further histological processing. The decalcified bones were embedded in paraffin and sections (4 µm) were cut and stained with hematoxylin and eosin (H&E) staining.

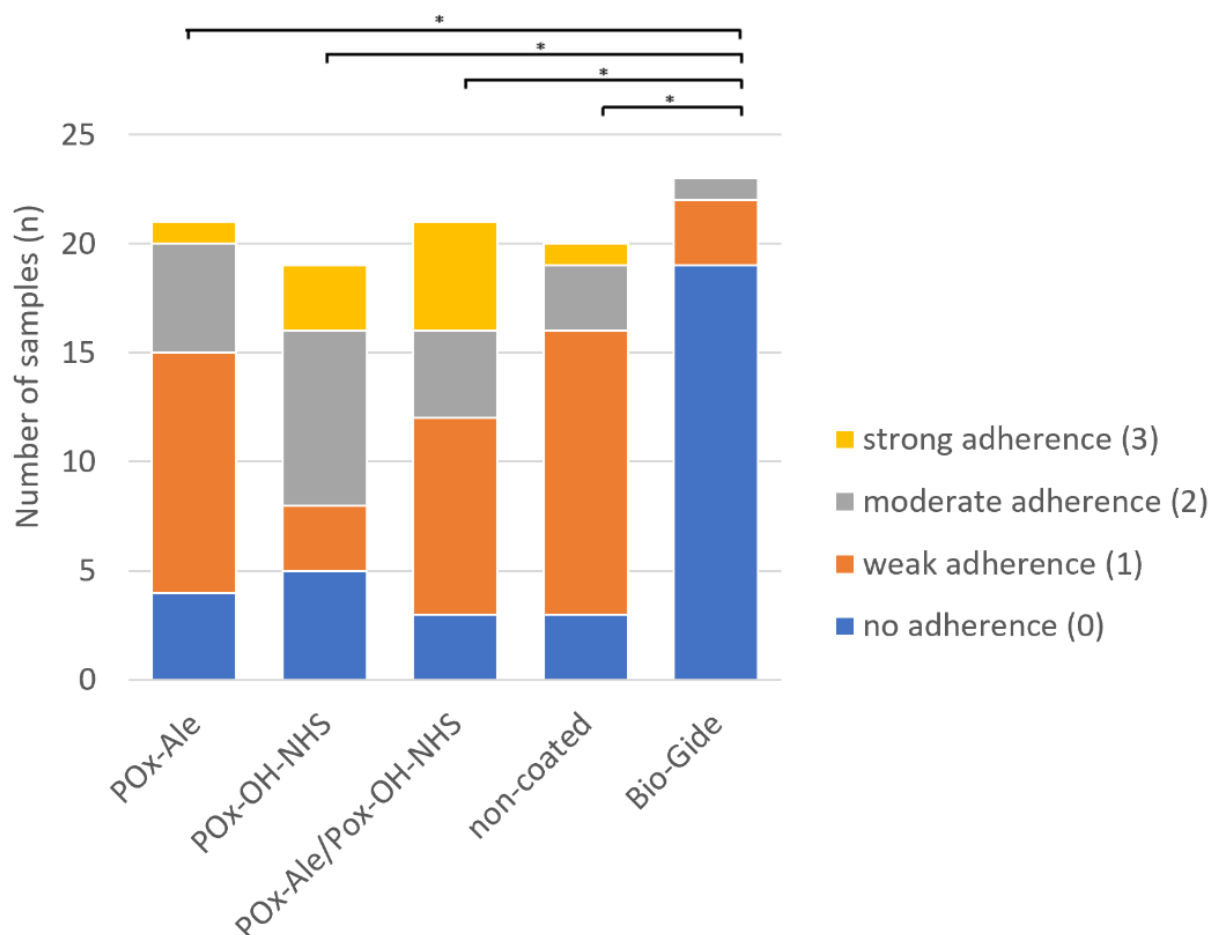


Fig. 3. Stacked bar graph of the scores for membrane adherence upon application per type of membrane. * A statistically significant difference ($p \leq 0.05$), calculated using a Kruskal-Wallis test compared between the experimental membranes and control membranes.

Outcomes and Measures

All outcomes and measures are presented in Table 1. All gradings were scored by two independent researchers. Directly after membrane application, adherence of the membrane towards bone tissue was graded by testing the movability of the membrane with tweezers. This score was introduced for the last 14 rats of the 5-day group and in all animals of the 14-day group. After sacrifice at day 5 or 14 post-operative, periosteum was scored for the presence of abscesses and redness, based on the scoring system used by Buyne *et al.* [28]. Subsequently, periosteum was opened and elevated, and the state of the membranes was assessed regarding coverage of the defect, detachment, swelling and displacement. In addition, tissue encapsulation was evaluated. The degree of adherence of the membrane to the tissues was graded during a peel off test and subsequently the cohesive strength of the membrane was scored, both based on score systems used in previous studies [22,23]. Histological sections were cut coronally through the midline of the defect and were assessed on newly formed bone and

soft tissue growth using a quantifiable grading scale similar to scales applied in literature [29–31]. Assessments for inflammatory cell infiltration were performed by scoring the percentage of inflammatory cells relative to the total cells in a histological section and by using an adjusted Ehrlich and Hunt numerical scale for the presence of immune cells at the biomaterial interface [32–36]. All histological samples were assessed by two independent blinded outcome assessors. When the assessors differed in grading, this was discussed until consensus on the grade was reached.

Data Analyses

Data was collected in Microsoft Excel and statistical analyses were performed using SPSS software (version 25, IBM, Armonk, NY, USA). Descriptive data were analysed by frequency distributions, presented as median with percentiles. Bias in defect location was assessed by comparing left with right defect outcomes. Moment scores (membrane performance and histological outcomes) of different membrane types were compared and to investigate the tempo-

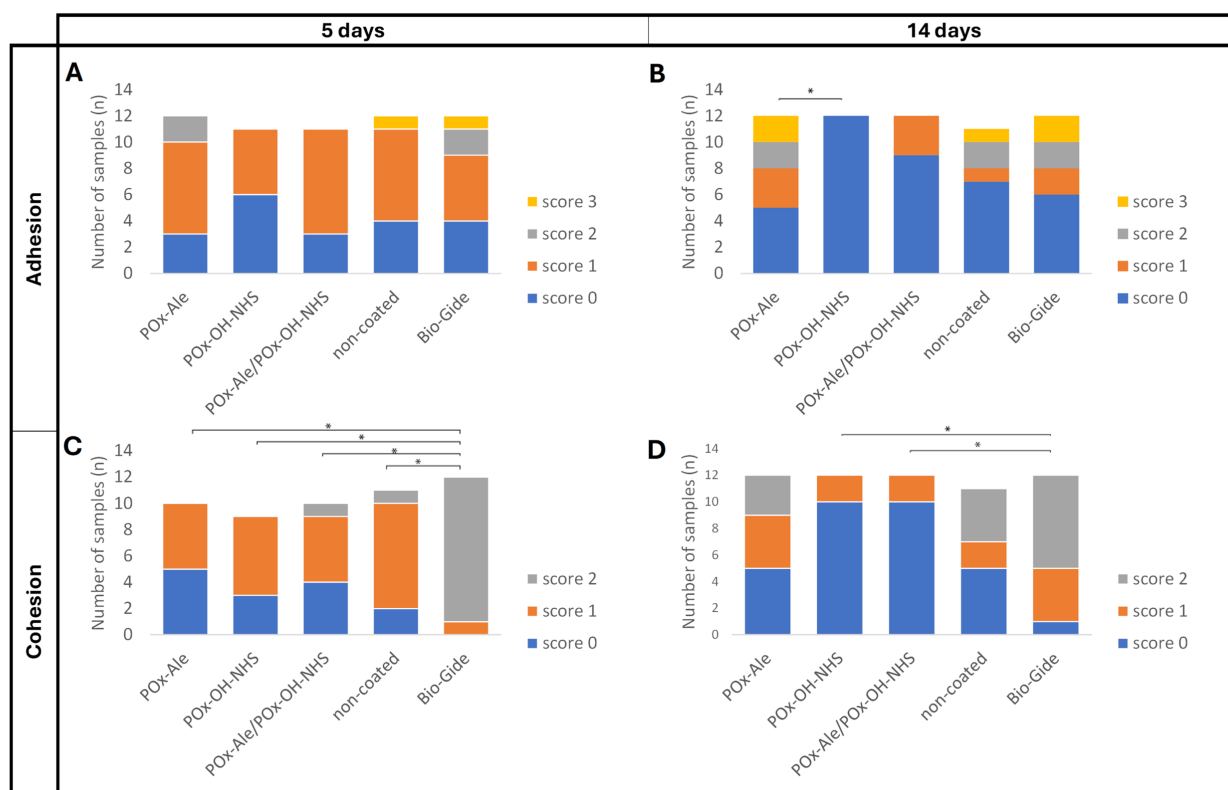


Fig. 4. Adhesion and cohesion scores. (A) Stacked bar graph of membrane adherence score at 5 days implantation per type of membrane. (B) Stacked bar graph of membrane cohesion score at 5 days implantation per type of membrane. Cohesive strength of the six membranes evaluated in the first three animals were not evaluated due to administrative issues. (C) Stacked bar graph of membrane adhesion score at 14 days implantation per type of membrane. (D) Stacked bar graph of membrane cohesion score at 14 days implantation per type of membrane. Statistical analysis calculated with Kruskal-Wallis test comparison between experimental and control membranes. *Statistically significant difference ($p \leq 0.05$).

ral effects, scores at day 5 and 14 were compared for each membrane type. A Kruskal-Wallis test with Bonferroni correction was used for ordinal data, and Fisher's exact test was used for ordinal data in comparisons of moment scores of the different membrane types (membrane performance and histological outcomes). Mann Whitney U test was used for nominal data and the Fisher's exact test was used for ordinal data in the comparison between the scores at day 5 and 14 for each membrane type.

Results

General Observations and Specimen Retrieval

One animal prematurely died approximately three hours after the surgical procedure (membrane POx-OH-NHS left defect, membrane POx-Ale/POx-OH-NHS right defect; Table 2), which was related to the general anaesthesia. The healing was uneventful for all other animals without postoperative complications in terms of abscesses, infections or signs of inflammation (swelling of the surgical site, redness of skin).

After 5 days, the periosteum completely covered the membrane upon sacrifice in all except one animal (POx-

Ale/POx-OH-NHS) (Fig. 2A). No abscesses, wound dehiscence or infections were observed in any of the animals. Two animals (POx-Ale membrane and POx-OH-NHS membrane, POx-Ale/POx-OH-NHS membrane and Bio-Gide membrane) showed signs of redness of a large part of the periosteum covering the membranes (score 2, moderate redness). Fibrous encapsulation was observed in one membrane (POx-Ale). One membrane (non-coated control) was detached and not covering the defect at sacrifice, and for nine membranes (three POx-Ale coated, three non-coated, two POx-OH-NHS, one POx-Ale/POx-OH-NHS) displacement was observed. None of the membranes showed visible signs of shrinking or tearing. Experimental membranes showed signs of fragmentation while this was not observed for Bio-Gide membranes (Fig. 2B).

No periosteal redness, wound dehiscence, infections or abscesses were observed in animals upon sacrifice at day 14. Except for three membranes (Bio-Gide, non-coated and POx-OH-NHS), all membranes were covered with a fibrous capsule that had formed cranially over the membranes (Fig. 2C). After 14 days, one membrane had detached (POx-Ale/POx-OH-NHS) and five membranes

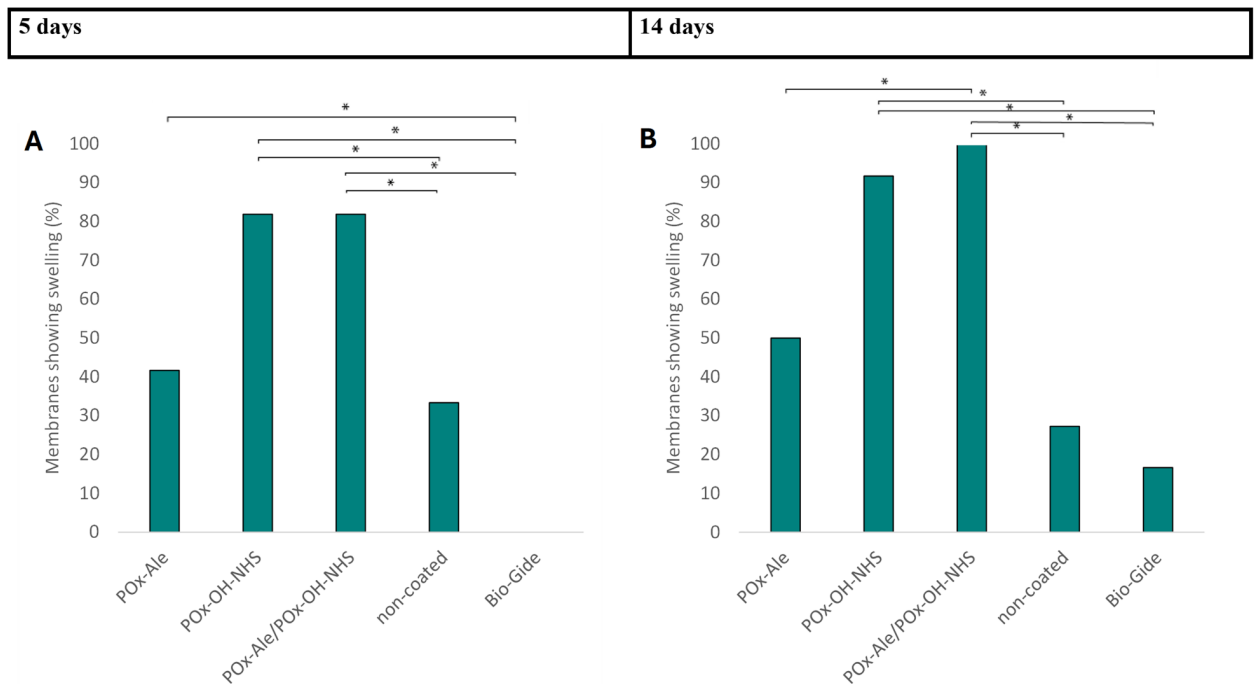


Fig. 5. Swelling scores. (A) Percentage of membranes showing membrane swelling after 5 days implantation per type of membrane. (B) Percentage of membranes showing membrane swelling after 14 days implantation per type of membrane. Statistical analysis calculated with Fisher's exact test comparison between experimental and control membranes. *Statistically significant difference ($p \leq 0.05$).

(three Bio-Gide, one POx-Ale/POx-OH-NHS, one non-coated) showed signs of displacement. In addition, one membrane (non-coated) was not retrieved upon sacrifice at day 14. None of the membranes showed visible signs of shrinking or tearing. No fragmentation of the Bio-Gide membrane was observed, while experimental membranes all showed signs of fragmentation similar to membranes at 5 days implantation.

Membrane Performance

Adhesion and Cohesion

No differences in initial membrane adherence between left and right cranial defects upon membrane application were found ($p = 0.962$). All experimental membranes showed a significantly higher adherence towards bone tissue upon application compared to control Bio-Gide membranes (median (mdn) 0.0 (0.0–0.0)), of which the highest median adhesion score was for POx-OH-NHS membranes (mdn 2.0 (0.0–2.0), $p = 0.000$) followed by POx-Ale/POx-OH-NHS (mdn 1.0 (1.0–2.5), $p = 0.000$), POx-Ale (mdn 1.0 (1.0–2.0), $p = 0.003$) and non-coated membranes (mdn 1.0 (1.0–1.0), $p = 0.006$) (Fig. 3).

Experimental membranes all showed “weak adherence” towards tissue at specimen retrieval at 5 days implantation (Fig. 4A), with median adherence scores of 1.0 (0.25–1.0) for POx-Ale membranes, 0.5 (0.0–1.0) for

POx-OH-NHS membranes and 1.0 (0.25–1.0) for POx-Ale/POx-OH-NHS membranes. No significant differences between experimental membranes and control membranes (non-coated (mdn 1.0 (0.0–1.0)) or Bio-Gide membranes (mdn 1.0 (0.0–1.75)) were found. Median cohesive strength scores were significantly higher for Bio-Gide membranes which scored “high cohesion strength” (mdn 2.0 (2.0–2.0)) compared to the “no adhesive strength” for POx-Ale membranes (mdn 0.5 (0.0–1.0), $p = 0.000$) and “medium cohesion” of POx-OH-NHS membranes (mdn 1.0 (0.0–1.0), $p = 0.001$), POx-Ale/POx-OH-NHS membranes (mdn 1.0 (0.0–1.0), $p = 0.001$, Fig. 4B).

Tissue adherence at 14 days implantation showed “no adherence” or “weak adherence” scores for the experimental membranes and control membranes, with medians of 1.0 (0.0–2.0) for POx-Ale, 0.0 (0.0–0.0) for POx-OH-NHS and 0.0 (0.0–0.75) for POx-Ale/POx-OH-NHS, and 0.0 (0.0–1.75) for non-coated membranes and 0.5 (0.0–2.0) for Bio-Gide membranes (Fig. 4C). Cohesion of Bio-Gide membranes (mdn 2.0 (2.0–2.0)) was significantly higher compared to POx-OH-NHS and POx-Ale/POx-OH-NHS membranes (mdn 0.0 (0.0–0.0) both membranes, $p = 0.000$) after 14 days, while POx-Ale (mdn 1.0 (0.0–1.75)) and non-coated membranes (mdn 1.0 (0.0–2.0)) scored “medium cohesion” (Fig. 4D).

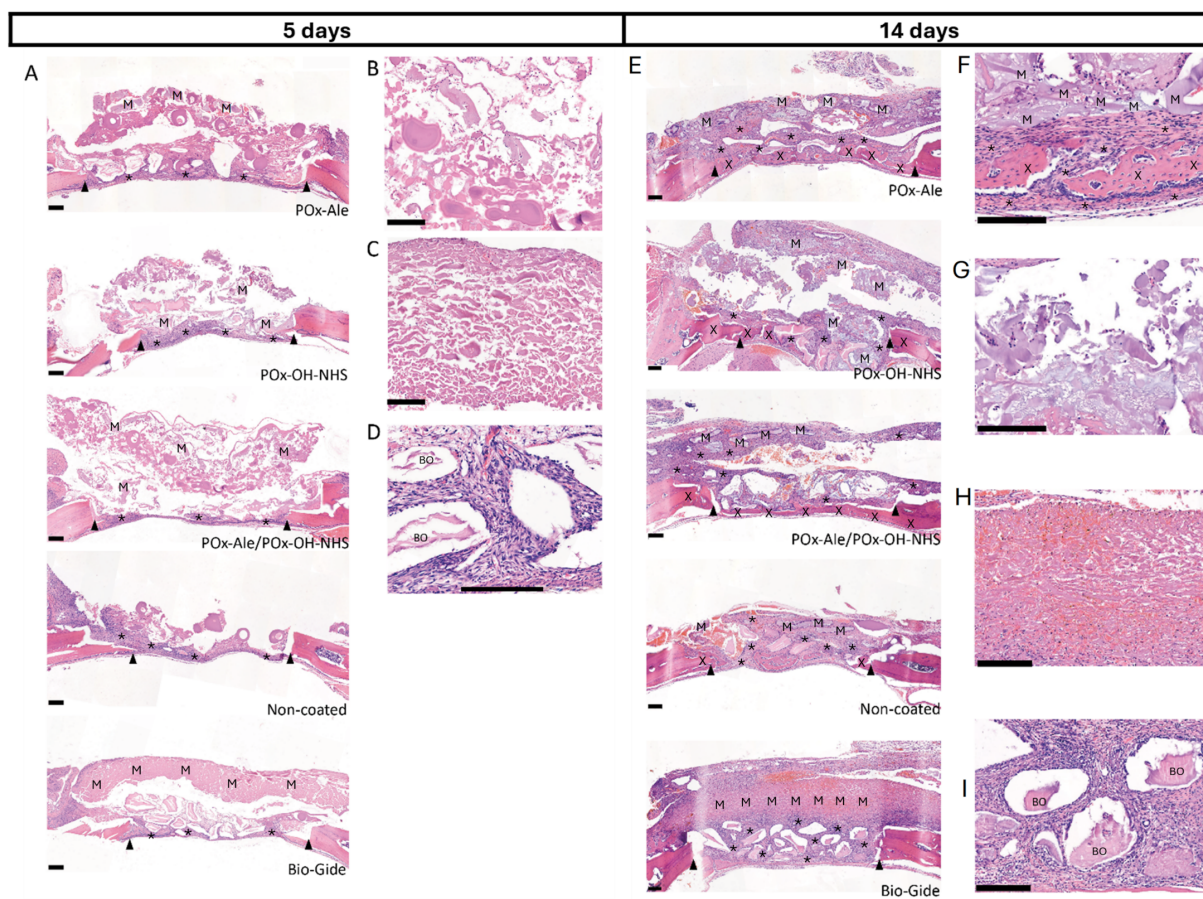


Fig. 6. Pictures of histological sections, coloured with H&E. Every picture is accompanied by a black bar representing 200 μ m. Arrows indicate the defect area, asterisks indicate soft tissue, X indicates neoformed bone, and M indicates membrane regions. (A) Representative images of histological sections at 5 days implantation, membranes POx-Ale, POx-OH-NHS, POx-Ale/POx-OH-NHS, non-coated control membrane and Bio-Gide® control membrane, respectively. (B) Representative image of the structure of experimental membrane at 5 days. (C) Representative image of the structure of Bio-Gide® membrane at 5 days. (D) Representative image of newly formed soft tissue in defect. (E) Representative images of histological sections at 14 days implantation, membranes POx-Ale, POx-OH-NHS, POx-Ale/POx-OH-NHS, non-coated control membrane and Bio-Gide® control membrane, respectively. (F) Representative image of newly formed bone. (G) Representative image of the structure of the experimental membrane at 14 days. (H) Representative image of the structure of Bio-Gide® membrane at 14 days. (I) Representative image of newly formed soft tissue in defect. BO, Bio-Oss. H&E, hematoxylin and eosin.

Swelling

After 5 days, swelling of the membranes was significantly more frequently observed for POx-Ale coated membranes ($p = 0.037$), POx-OH-NHS ($p = 0.000$) and POx-Ale/POx-OH-NHS-coated membranes ($p = 0.000$) membranes compared to Bio-Gide membranes (Fig. 5A). In addition, POx-OH-NHS and POx-Ale/POx-OH-NHS-coated membranes showed more macroscopic membrane swelling compared to non-coated membranes ($p = 0.036$ and $p = 0.036$, respectively). After 14 days, membrane swelling was significantly more frequently observed for POx-OH-NHS ($p = 0.003$ and $p = 0.001$) and POx-Ale/POx-OH-NHS-coated membranes ($p = 0.000$ and $p = 0.000$) compared to non-coated membranes and Bio-Gide membranes, respectively (Fig. 5B).

Histological Observations

General Observations

Eight tissue samples were not assessed histologically since these samples were lost during histological processing caused by technical issues. These samples included one POx-Ale membrane, two POx-OH-NHS membranes, one POx-Ale/POx-OH-NHS membrane, one non-coated membrane, one Bio-Gide membrane (day 5), one POx-OH-NHS and one POx-Ale/POx-OH-NHS membrane (day 14, Table 2).

Light microscopical analysis of the 5 days implantation specimens showed similar tissue healing in all specimens (Fig. 6A). The bone defect margins could be clearly discerned. In most specimens, soft tissue containing connective tissue fibroblasts and inflammatory cell infiltra-

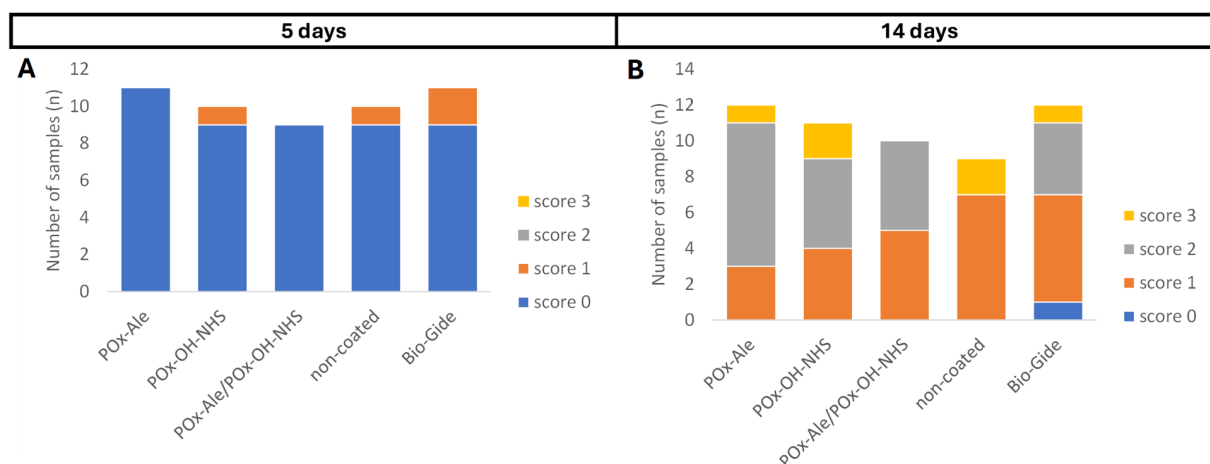


Fig. 7. Neoformed bone scores. (A) Stacked bar graph of newly formed bone score at 5 days implantation per type of membrane. (B) Stacked bar graph of newly formed bone score at 14 days implantation per type of membrane.

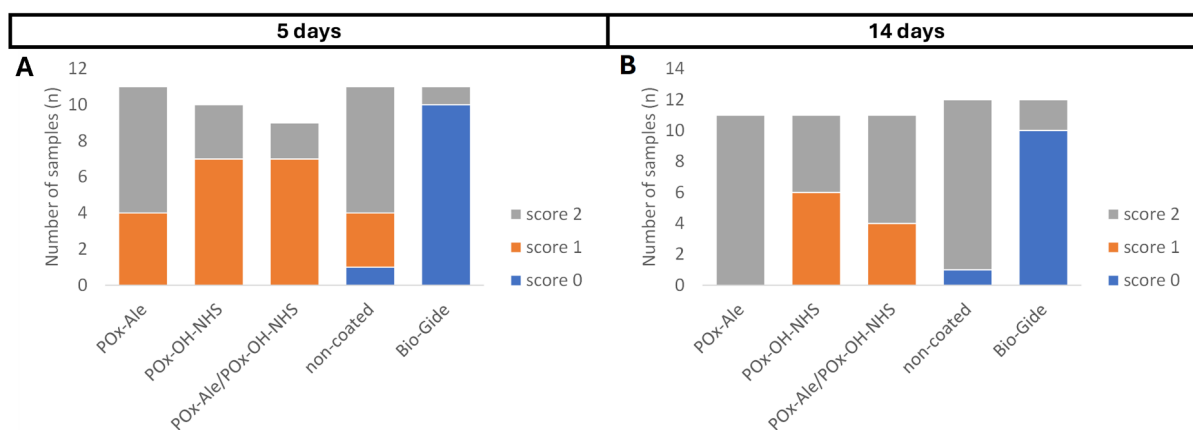


Fig. 8. Membrane degradation scores. (A) Stacked bar graph of membrane degradation score at 5 days implantation per type of membrane. (B) Stacked bar graph of membrane degradation score at 14 days implantation per type of membrane. Statistical analyses are calculated using Kruskal-Wallis test comparison between experimental and control membranes.

tion was bridging the defects at the side of the dura mater. Membrane structures were always visible on top/in the defect areas. All experimental- and non-coating membranes showed open and disintegrated membrane structures (Fig. 6B) in comparison with the denser Bio-Gide membranes (Fig. 6C). In the majority of the specimens, Bio-Oss granules were identified which were often enclosed by nucleirich fibrous tissue (Fig. 6D).

Light microscopical analysis of the 14-day implantation specimens showed comparable tissue- and bone regeneration in all treatment groups (Fig. 6E). Defect areas were filled with soft tissue mainly containing fibroblasts and inflammatory cells. Membranes were present on top of the defects and covered with a fibrous layer. Newly formed bone tissue was present at the borders of the defects and in six defects complete bridging of the bone at the bottom of the defect was visible. New bone (woven) was present in all specimens (Fig. 6F), except one specimen which was

covered with a Bio-Gide membrane. All experimental- and non-coating membranes consisted of more open and disintegrated membrane structures as seen in Fig. 6G. Bio-Gide membranes showed a dense membrane structure similar to its structure after 5 days (Fig. 6H). In some of the specimens, Bio-Oss particles were visible, enclosed by a dense layer of fibrous tissue (Fig. 6I).

Bone Growth

No significant differences in bone growth scores between the membrane types were present after 5 days (Fig. 7A). In four specimens (1 × POx-OH-NHS, 1 × non-coated, and 2 × Bio-Gide), limited newly formed bone was present while in the other specimens no bone formation was visible. After 14 days, median neobone formation scores ranged from 1 (bony bridging only at defect borders) for non-coated and commercial Bio-Gide membranes (mdn 1.0 (1.0–2.0), both) and POx-Ale/POx-OH-NHS (mdn 1.5

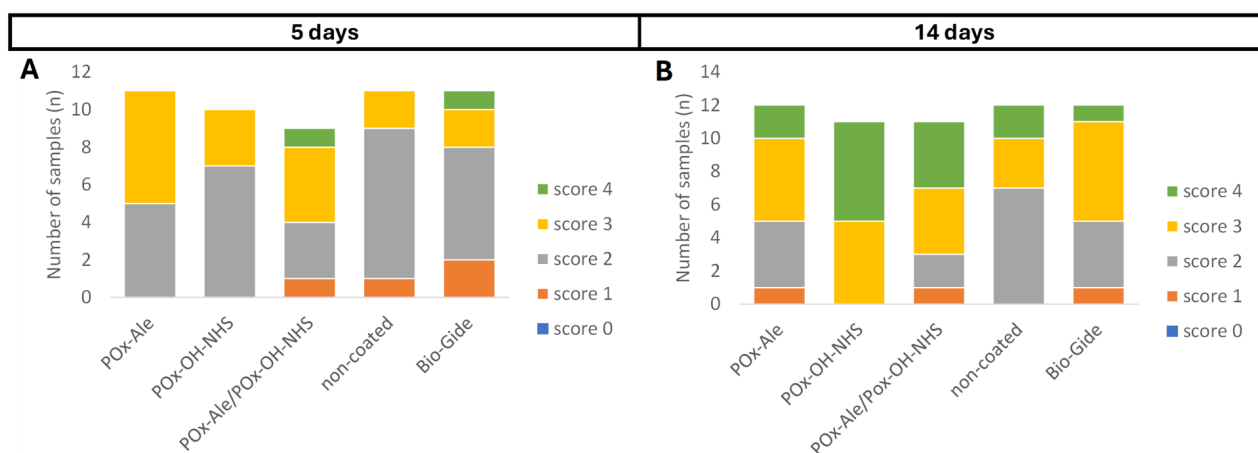


Fig. 9. Inflammatory cell infiltration scores. (A) Stacked bar graph of inflammatory cell infiltrate score at 5 days implantation per type of membrane. (B) Stacked bar graph of inflammatory cell infiltrate score at 14 days implantation per type of membrane. Statistical analyses are calculated using Kruskal-Wallis test comparison between experimental and control membranes.

(1.0–2.0) to 2 (bony bridging over partial length of defect) for POx-OH-NHS (mdn 2.0 (1.0–2.0)) and POx-Ale membranes (mdn 2.0 (1.25–2.0, Fig. 7B)). Differences between highest (POx-Ale and POx-OH-NHS) and lowest amount of bone regeneration (Bio-Gide) were non-significant ($p = 0.447$). Except from one defect (14 days, POx-Ale membrane), soft tissue was completely bridging the defect (score 3) or filling the entire span and depth of the defect (score 4) in all animals. No differences regarding bone formation were observed between the different membrane types or implantation periods.

Membrane Degradation

Membrane fragmentation was observed in all membranes, showing a significant faster degradation of POx-Ale (mdn 2.0 (1.0–2.0), $p = 0.000$) and POx-OH-NHS (mdn 1.0 (1.0–2.0), $p = 0.023$) membranes compared to commercial Bio-Gide membranes (mdn 0.0 (0.0–0.0)) of which the latter showed almost intact membranes after 5 days implantation (Fig. 8A). After 14 days, membrane degradation scores were low for Bio-Gide membranes (mdn 0.0 (0.0–0.0); Fig. 8B) while POx-Ale (mdn 2.0 (2.0–2.0), $p = 0.014$) and POx-Ale/POx-OH-NHS (mdn 2.0 (1.0–2.0), $p = 0.000$) membranes showed signs of severe fragmentation of the membranes. In none of the membrane types were significant differences found in degradation state between 5 and 14 days.

Inflammatory Cell Infiltration

After 5 days, inflammatory cell infiltrate was present in the defect areas with percentages ranging from 26–50 % (score 2) for membranes coated with POx-OH-NHS (mdn 2.0 (2.0–3.0)), non-coated control membranes (mdn 2.0 (2.0–2.0)) and Bio-Gide membranes (mdn 2.0 (2.0–3.0)), to 51–75 % (score 3) for POx-Ale (mdn 3.0 (2.0–3.0)) and POx-Ale/POx-OH-NHS (mdn 3.0 (2.0–3.0)) membranes (Fig. 9A). After 14 days, the extent of inflama-

tory infiltrate was similar to measurements after 5 days for all membrane types (26–75 %), except for POx-OH-NHS-coated membranes which showed a higher inflammatory cell infiltrate (mdn 4.0 (3.0–4.0, $p = 0.000$)), and which was significantly higher compared to non-coated membranes (mdn 2.0 (2.0–3.0), $p = 0.047$; Fig. 9B). No differences between the coated membranes and control membranes were found, nor were differences between the membranes found with the Ehrlich & Hunt scale.

Discussion

In the present study, the bone adherence and short-term biocompatibility of novel tissue adhesive barrier membranes were investigated in a rat cranial defect model toward facilitation of barrier membrane application and improved bone regeneration. Experimental membranes with a tissue adhesive coating showed a significantly higher bone adherence upon membrane application compared to commercial Bio-Gide membranes, and animals treated with experimental membranes showed similar tissue healing. Bone formation was found in almost all defect sites after 14 days. However, degradation of the experimental membranes led to fragmentation from 5 days postoperatively.

Membranes and tissue responses were evaluated after 5 days, when inflammatory reactions in wound healing should be highly present and visible, and at 14 days postoperative when the first inflammatory responses in a normal healing process should have disappeared [37,38]. At these timepoints, when reactions are eminent, differences are most distinct and clearly visible. However, hardly any major changes between inflammatory cell infiltrate between the two timepoints were observed, regardless of membrane types. No excessive inflammatory reactions or postoperative complications were present in any of the animals, suggesting mild tissue responses. Superficial fibrous capsules

formed cranially over the membranes to isolate the foreign material from the body were present for all membrane types after 14 days and this corroborates observations in previous studies with (commercial) barrier membranes [37,39,40]. These foreign body reactions have been described as “bioincompatible” processes and might be responsible for accelerated degradation of the biomaterial and impeded healing of the bone defect [41,42]. In contrast, others have postulated advantages of the fibrous layer over the biomaterial since it allows integration with the connective tissues [14].

As hypothesized, the addition of POx-polymer coatings enhanced the adherence of the membrane toward bone tissue, which kept the membranes in place immediately upon application and during wound closure, and hence improved its handling properties. Adherence to bone tissue ensures stability of the membrane and minimizes membrane movement, which prevents soft tissue ingrowth and stimulates bone regeneration [43]. Recent studies showed tissue binding and haemostatic properties of POx-OH-NHS polymer in combination with gelatine membrane base layer as used in the present study [19,21]. The cross-links between the POx-OH-NHS polymer and the gelatine layer, blood proteins and tissues containing amines create a gel which adheres to the tissue surface. In *in vivo* and perfusion-based *ex vivo* studies using pig models containing blood, similar adhesive performance of the POx-OH-NHS coatings were observed [23].

POx-Ale-coated membranes bind by a bone-specific bonding with the calcium content in bone tissue mineral. These bone binding characteristics were demonstrated in previous *in vitro*, *ex vivo* and *in vivo* studies [22,23]. Similar to our previous *ex vivo* study [44], we here found an enhanced but less strong adherence of POx-Ale-coated membranes in relation to POx-OH-NHS membranes. Strikingly, non-coated experimental membranes also showed significantly enhanced adhesive properties towards bone tissue probably caused by the naturally adhesive properties of the gelatine base of the membrane [10,45]. Furthermore, the collagen from Bio-Gide membranes should have a minor adhesive capacity with blood coagulation, which we hardly observed in the assessments directly after membrane application. In a situation when the bleeding is more intense and more blood is in contact with the membrane, or when there is more time between membrane application and assessment, some weak or moderate adherence for the Bio-Gide membranes should be expected.

After implantation periods of 5 or 14 days, differences in adherence as seen during application diminished as most membranes did not move from the wound region. Adherence with the surrounding soft tissues were observed, which complicated discrimination of soft tissue adherence vs. adherence toward bone tissue. A significantly higher tissue adherence of POx-Ale membranes in comparison with POx-OH-NHS membranes was found after implantation, but the relationship between the coating of the membrane

and the adherence to tissues after implantation is not clear yet.

A reasonable amount of bone regeneration was present in the cranial defects after 14 days of implantation. In some defects, the newly formed bone was bridging the entire defect, which exceeded results in another study using this model and given the age of the rats [46]. Although alendronate might have bone growth-stimulating properties related to its anti-osteoclastic efficacy [47,48], no clear improvements in bone growth were observed for membranes coated with alendronate-functionalized polymer. Newly formed bone in defects treated with experimental membranes was comparable with the commercial Bio-Gide membranes of which biocompatibility has already been proven [49,50], indicating a similar biocompatibility with bone and surrounding tissues.

Both macroscopic and histological evaluation showed that the cohesive strength of the experimental membrane structures was significantly weaker compared to Bio-Gide membranes. In addition, the degradation of the experimental membranes had strongly advanced after 5 days. However, further fragmentation was not visible after 14 days. Assuming a clinically relevant degradation time of at least 6 weeks for barrier membranes to maintain a barrier function, the here observed degradation for the experimental membranes is likely too fast, which might contribute to a faster and more extensive resorption of bone tissue [41]. Swelling of the membranes as seen in the coated and non-coated experimental types might result in compression on the surrounding tissues or exposure of the membrane to the oral cavity which should be avoided [51]. Furthermore, it might weaken the interfacial adherence of the membranes [22]. The membrane swelling may be caused by the behavior of the membrane base which consists of several compressed layers of gelatine-based fibrillar. Bio-Gide membranes are denser compared to the experimental membranes, and this leads to a reduced swelling pattern in the commercial Bio-Gide membranes. Therefore, different types of membranes for POx-polymer coating should be considered for guided bone regeneration applications, preferably absorbable materials including (crosslinked) collagen as well as synthetic materials such as (combinations of) polylactic acid and trimethyl chitosan known to have appropriate mechanical properties [52].

Although this study proved the adhesive bone-promoting of the POx-Ale and/or POx-OH-NHS coated gelatine membranes in the bilateral cranial defect model, further studies must be performed to optimize the membranes for clinical application. Ideally, studies on the coating or impregnation of the POx-polymers on different materials should be performed to develop tissue adhesive membranes with membrane base layers which already proved their high standard of mechanical, (low) swelling and biodegradable characteristics in a clinical setting. Experiments should also be performed on different composi-

tions of the POx-polymers and/or additional components (i.e., bone bio-adhesives or nano glues) to find the ideal configuration for the consolidation of the membrane with the bone tissue. Subsequently, long term studies should be performed in which the barrier efficacy, feasibility and biocompatibility of the membranes will be investigated until full thickness bone regeneration. For these studies, critical defect models in large animals should be used that simulate more challenging and clinically relevant circumstances including the bacterial microbiome of the oral environment and the movements of the maxillofacial area [53].

The use of a non-critical cranial defect of 4 mm diameter limits the result interpretation in this study, as comparable studies on guided bone regeneration have used critical- or larger defect models [27,43,46]. We chose this model because of the accessibility of the bone tissue and minimal risk of damage to surrounding vital tissues, which decreases the chances of postoperative complications and facilitated the evaluation of different treatment options. Also, this model closely resembles maxillofacial bone remodeling and the non-weight-bearing character minimizes the extent of load and associated challenges in the application area [54,55]. Moreover, our focus for this study was to compare the experimental membranes on their *in vivo* tissue adhesion capabilities. For further investigation, it is advised to further examine the novel membrane's effect on bone healing in a critical defect model for a longer period. Furthermore, the usage of an animal model more resembling the clinical situation would provide for more reliable outcomes.

A broader comparison could enhance the evaluation of the experimental membranes' performance. Currently, different types of resorbable membranes that are used in clinical practice consist of natural membranes made from collagen type I and III, chitosan, or acellular dermal matrix, and synthetic membranes made from polyglycolic acid, poly-L-lactic acid, or poly- ϵ -caprolactone [14,56]. Multiple studies in human and animal subjects have been conducted that compared the effectiveness of these membrane types, with Bio-Gide, our choice as positive control group, seemingly performing the best out of all membranes tested [43,57–59]. Further, the clinical efficacy of Bio-Gide has been validated through numerous clinical trials and -studies [60–63]. We deemed the direct comparison of our membrane prototypes with one well-investigated membrane sufficient for this initial study, also to avoid unjustified use of a high number of animals [64]. After selecting one or two best-performing membrane prototypes, an effectiveness study has to be performed that should include multiple positive control membranes.

Interpretation of histological scoring utilized in this study should be done with caution due to several inherent limitations. We made use of grading scales to provide quantifiable histological outcomes. It is known that a reproducible and meaningful scoring system is a cost-effective method that improves the robustness of histolog-

ical outcome evaluation [65]. To minimize observer bias, the grading in this study was performed by two independent, blinded outcome assessors. Still, it remains a challenge to set up a scoring system that represents a true linear relationship between grades [66,67]. The histological scoring system was deemed adequate for this study, given that histological analysis was not our primary aim. Long-term studies focused on membrane biocompatibility and -degradability would benefit from objective automated imaging analysis techniques, thereby increasing the study's rigor with reproducible reliable data [27,68].

The short evaluation period of 5 and 14 days in this study provides clear signs but is insufficient for drawing definite conclusions about membrane stability, -degradability and -tissue integration. Also, this study did not detail the molecular mechanisms underlying bone regeneration and tissue response to the membranes. Analyses such as immunohistochemical evaluation, assays on osteoblast- and fibroblast proliferation using molecular markers or real-time quantitative polymer chain reaction (RT-qPCR), and the chemical characterization of degradational products through analytical techniques (e.g., high-performance liquid chromatography, nuclear magnetic resonance, Fourier-transform infrared spectroscopy) could enrich our current understanding of all biological processes involved [69,70]. Utilizing these analyses in this study was deemed unjustified because the primary study aim was to determine the adhesion capabilities and short-term biocompatibility of the experimental membranes, in comparison to a commercial standard and a non-coated control membrane. It is recommended that future studies of one or two best-performing experimental membranes include several of the aforementioned analytical techniques and a longer evaluation period, to obtain a more complete understanding of the biological mechanisms that are involved in the implantation and degradation of these POx membranes. Such a long-term effectiveness- and safety study warrants a high number of animals, in accordance with current ethical considerations of animal studies [24,64].

Conclusions

This study investigated the adherence efficacy and short-term biocompatibility of novel bone adhesive barrier membranes for guided bone regeneration. The addition of POx-polymer coatings did enhance the adherence of the membranes towards bone tissue, which is beneficial for application of these membranes. Similar tissue healing was observed in defects treated with bone adhesive barrier membranes compared to commercial Bio-Gide membrane, but fast fragmentation of the bone adhesive membranes stresses that different membrane base layers should be used. Overall, the POx-polymer coating holds promise as an effective coating for barrier membrane for guided bone regeneration procedures, in which it prevents membrane collapse or -dislocation and improves implant stability.

List of Abbreviations

GBR, guided bone regeneration; POx, poly(2-oxazoline); Ale, alendronate; OH-NHS, *N*-hydroxysuccinimide; H&E, hematoxylin and eosin; mdn, median.

Availability of Data and Materials

The data that support the findings of this study are available from the corresponding author (SP) upon reasonable request.

Author Contributions

MvE, BvO, RFL, HvG and SL contributed to the design of this work. HvG, SP, SL, BvO, RFL and JvdB contributed to the interpretation of data. SP and MvE analyzed the data and drafted the manuscript. HvG, SL and JvdB revised critically and supervised the manuscript. All authors read and approved the final manuscript. All authors agreed to be accountable for all aspects of the work in ensuring that questions related to the accuracy or integrity of any part of the work were appropriately investigated and resolved.

Ethics Approval and Consent to Participate

The study was approved by the Dutch Animal Ethics Committee (project number 2020-0016).

Acknowledgments

We are grateful to the staff of the Central Animal Laboratory for their technical assistance and advice in the animal studies. We would like to thank Roger Lomme, Nicole Calon and Sjors van Schijndel of the department of surgery, and Natasja van Dijk and Vincent Cuijpers of the Regenerative Biomaterials group for their expertise and support during the animal experiments and histological analyses.

Funding

This work was supported by the Netherlands Organization for Scientific Research (NWO, grant No. 14435) and GATT Technologies BV.

Conflict of Interest

Sander Leeuwenburgh and Harry van Goor were scientific advisors of GATT Technologies BV until 31 December 2021, Steven Poos and Rosa Félix Lanao are employees of GATT Technologies BV.

References

- [1] Le Guéhennec L, Soueidan A, Layrolle P, Amouriq Y. Surface treatments of titanium dental implants for rapid osseointegration. *Dental Materials: Official Publication of the Academy of Dental Materials*. 2007; 23: 844–854. <https://doi.org/10.1016/j.dental.2006.06.025>.
- [2] Albrektsson T, Wennerberg A. On osseointegration in relation to implant surfaces. *Clinical Implant Dentistry and Related Research*. 2019; 21: 4–7. <https://doi.org/10.1111/cid.12742>.
- [3] Javed F, Ahmed HB, Crespi R, Romanos GE. Role of primary stability for successful osseointegration of dental implants: Factors of influence and evaluation. *Interventional Medicine & Applied Science*. 2013; 5: 162–167. <https://doi.org/10.1556/IMAS.5.2013.4.3>.
- [4] Gil J, Sandino C, Cerrolaza M, Pérez R, Herrero-Climent M, Rios-Carrasco B, *et al*. Influence of Bone-Level Dental Implants Placement and of Cortical Thickness on Osseointegration: In Silico and In Vivo Analyses. *Journal of Clinical Medicine*. 2022; 11: 1027. <https://doi.org/10.3390/jcm11041027>.
- [5] Chan HL, Lin GH, Fu JH, Wang HL. Alterations in bone quality after socket preservation with grafting materials: a systematic review. *The International Journal of Oral & Maxillofacial Implants*. 2013; 28: 710–720. <https://doi.org/10.11607/jomi.2913>.
- [6] Pagni G, Pellegrini G, Giannobile WV, Rasperini G. Postextraction alveolar ridge preservation: biological basis and treatments. *International Journal of Dentistry*. 2012; 2012: 151030. <https://doi.org/10.1155/2012/151030>.
- [7] Omar O, Elgali I, Dahlin C, Thomsen P. Barrier membranes: More than the barrier effect? *Journal of Clinical Periodontology*. 2019; 46: 103–123. <https://doi.org/10.1111/jcpe.13068>.
- [8] Needleman I, Tucker R, Giedrys-Leeper E, Worthington H. A systematic review of guided tissue regeneration for periodontal infrabony defects. *Journal of Periodontal Research*. 2002; 37: 380–388. <https://doi.org/10.1034/j.1600-0765.2002.01369.x>.
- [9] Liu J, Kerns DG. Mechanisms of guided bone regeneration: a review. *The Open Dentistry Journal*. 2014; 8: 56–65. <https://doi.org/10.2174/1874210601408010056>.
- [10] Wang X, Zhu J, Liu X, Zhang HJ, Zhu X. Novel Gelatin-based Eco-friendly Adhesive with a Hyperbranched Cross-linked Structure. *Industrial & Engineering Chemistry Research*. 2020; 59: 5500–5511. <https://doi.org/10.1021/acs.iecr.9b06822>.
- [11] Amano Y, Ota M, Sekiguchi K, Shibukawa Y, Yamada S. Evaluation of a poly-L-lactic acid membrane and membrane fixing pin for guided tissue regeneration on bone defects in dogs. *Oral Surgery, Oral Medicine, Oral Pathology, Oral Radiology, and Endodontics*. 2004; 97: 155–163. <https://doi.org/10.1016/j.tripleo.2003.09.009>.
- [12] ElHawary H, Baradaran A, Abi-Rafeh J, Vorstenbosch J, Xu L, Efanov JI. Bone Healing and Inflammation: Principles of Fracture and Repair. *Seminars in Plastic Surgery*. 2021; 35: 198–203. <https://doi.org/10.1055/s-0041-1732334>.
- [13] Nyary T, Scammell BE. Principles of bone and joint injuries and their healing. *Surgery (Oxford)*. 2018; 36: 7–14. <https://doi.org/10.1016/j.mpsur.2017.10.005>.
- [14] Dimitriou R, Mataliotakis GI, Calori GM, Giannoudis PV. The role of barrier membranes for guided bone regeneration and restoration of large bone defects: current experimental and clinical evidence. *BMC Medicine*. 2012; 10: 81. <https://doi.org/10.1186/1741-7015-10-81>.
- [15] Elgali I, Omar O, Dahlin C, Thomsen P. Guided bone regeneration: materials and biological mechanisms revisited. *European Journal of Oral Sciences*. 2017; 125: 315–337. <https://doi.org/10.1111/eos.12364>.
- [16] Pulikkotil SJ, Nath S. Use of Fibrin Sealant in Guided Tissue Regeneration of Intrabony Defect. *JBR Journal of Interdisciplinary Medicine and Dental Science*. 2015; 3. https://www.researchgate.net/publication/275225902_Use_of_Fibrin_Sealant_in_Guided_Tissue_Regeneration_of_Intrabony_Defect.
- [17] Bhagat V, Becker ML. Degradable Adhesives for Surgery and Tissue Engineering. *Biomacromolecules*. 2017; 18: 3009–3039. <https://doi.org/10.1021/acs.biomac.7b00969>.
- [18] Norton MR, Kay GW, Brown MC, Cochran DL. Bone glue—The final frontier for fracture repair and implantable device stabilization. *International Journal of Adhesion and Adhesives*. 2020; 102: 102647–102654. <https://doi.org/10.1016/j.ijadhadh.2020.102647>.
- [19] Boerman MA, Roozen E, Sánchez-Fernández MJ, Keereweer AR, Félix Lanao RP, Bender JCME, *et al*. Next Generation Hemostatic Materials Based on NHS-Ester Functionalized Poly(2-oxazoline)s.

- Biomacromolecules. 2017; 18: 2529–2538. <https://doi.org/10.1021/acs.biomac.7b00683>.
- [20] Sánchez-Fernández MJ, Immers MR, Félix Lanao RP, Yang F, Bender JCME, Mecinović J, *et al.* Alendronate-Functionalized Poly(2-oxazoline)s with Tunable Affinity for Calcium Cations. *Biomacromolecules*. 2019; 20: 2913–2921. <https://doi.org/10.1021/acs.biomac.9b00104>.
- [21] Roozen EA, Warlé MC, Lomme RMLM, Félix Lanao RP, van Goor H. New polyoxazoline loaded patches for hemostasis in experimental liver resection. *Journal of Biomedical Materials Research. Part B, Applied Biomaterials*. 2022; 110: 597–605. <https://doi.org/10.1002/jbm.b.34938>.
- [22] Sánchez-Fernández MJ, Peerlings M, Félix Lanao RP, Bender JCME, van Hest JCM, Leeuwenburgh SCG. Bone-adhesive barrier membranes based on alendronate-functionalized poly(2-oxazoline)s. *Journal of Materials Chemistry. B*. 2021; 9: 5848–5860. <https://doi.org/10.1039/d1tb00502b>.
- [23] van Erk M, Lomme R, Sánchez-Fernández MJ, van Oirschot BAJA, Félix Lanao RP, Leeuwenburgh SCG, *et al.* Novel alendronate and NHS-ester functionalized poly(2-oxazoline)s bone adhesive barrier membranes for guided bone regeneration: Prototype selection and experimental model comparison. *Materialia*. 2022; 24: 101517–101524. <https://doi.org/10.1016/j.mtl.2022.101517>.
- [24] Percie du Sert N, Ahluwalia A, Alam S, Avey MT, Baker M, Browne WJ, *et al.* Reporting animal research: Explanation and elaboration for the ARRIVE guidelines 2.0. *PLoS Biology*. 2020; 18: e3000411. <https://doi.org/10.1371/journal.pbio.3000411>.
- [25] Smith AJ. Guidelines for planning and conducting high-quality research and testing on animals. *Laboratory Animal Research*. 2020; 36: 21. <https://doi.org/10.1186/s42826-020-00054-0>.
- [26] International Organization for Standardization. ISO/TC 194. ISO10993-6:2016 Biological evaluation of medical devices — Part 6: Tests for local effects after implantation. 2016. Available at: <https://cdn.standards.iteh.ai/samples/61089/a92afde82feb4be886970ccc3e250033/ISO-10993-6-2016.pdf> (Accessed: 5 September 2024).
- [27] Araújo LK, Lopes MS, Souza FFP, Melo MM, Paulo AO, Castro-Silva IL. Efficiency analysis of commercial polymeric membranes for bone regeneration in rat cranial defects. *Acta Cirúrgica Brasileira/Sociedade Brasileira para Desenvolvimento Pesquisa em Cirurgia*. 2023; 38: e380623. <https://doi.org/10.1590/acb380623>.
- [28] Buyné OR, Bleichrodt RP, De Man BM, Lomme RM, Verweij PE, van Goor H, *et al.* Tissue-type plasminogen activator prevents abscess formation but does not affect healing of bowel anastomoses and laparotomy wounds in rats with secondary peritonitis. *Surgery*. 2009; 146: 939–946. <https://doi.org/10.1016/j.surg.2009.04.028>.
- [29] Patel ZS, Young S, Tabata Y, Jansen JA, Wong MEK, Mikos AG. Dual delivery of an angiogenic and an osteogenic growth factor for bone regeneration in a critical size defect model. *Bone*. 2008; 43: 931–940. <https://doi.org/10.1016/j.bone.2008.06.019>.
- [30] Wang Z, Hui A, Zhao H, Ye X, Zhang C, Wang A, *et al.* A Novel 3D-bioprinted Porous Nano Attapulgit Scaffolds with Good Performance for Bone Regeneration. *International Journal of Nanomedicine*. 2020; 15: 6945–6960. <https://doi.org/10.2147/IJN.S254094>.
- [31] Gokyer S, Monsef YA, Buyuksungur S, Schmidt J, Vladescu Dragomir A, Uygur S, *et al.* MgCa-Based Alloys Modified with Zn- and Ga-Doped CaP Coatings Lead to Controlled Degradation and Enhanced Bone Formation in a Sheep Cranium Defect Model. *ACS Biomaterials Science & Engineering*. 2024; 10: 4452–4462. <https://doi.org/10.1021/acsbiomaterials.4c00358>.
- [32] Phillips JD, Kim CS, Fonkalsrud EW, Zeng H, Dindar H. Effects of chronic corticosteroids and vitamin A on the healing of intestinal anastomoses. *American Journal of Surgery*. 1992; 163: 71–77. [https://doi.org/10.1016/0002-9610\(92\)90255-p](https://doi.org/10.1016/0002-9610(92)90255-p).
- [33] Calisir A, Ece I, Yormaz S, Colak B, Kirazli H, Sahin M. The Effects of Platelet-Rich Plasma to Decrease the Risk of Seroma Formation After Mastectomy and Axillary Dissection. *The Journal of Surgical Research*. 2020; 256: 156–162. <https://doi.org/10.1016/j.js.s.2020.06.037>.
- [34] Ceran C, Aksoy RT, Gülbahar O, Öztürk F. The effects of ghrelin on colonic anastomosis healing in rats. *Clinics*. 2013; 68: 239–244. [https://doi.org/10.6061/clinics/2013\(02\)oa19](https://doi.org/10.6061/clinics/2013(02)oa19).
- [35] Özkececi ZT, Gonul Y, Karavelioglu A, Bozkurt MF, Kacar E, Bal A, *et al.* The effect of enoxaparin on seroma and mesh-tissue adhesion in a hernia model. *Clinical and Experimental Pharmacology & Physiology*. 2016; 43: 690–697. <https://doi.org/10.1111/1440-1681.12582>.
- [36] Ehrlich HP, Tarver H, Hunt TK. Effects of vitamin A and glucocorticoids upon inflammation and collagen synthesis. *Annals of Surgery*. 1973; 177: 222–227. <https://doi.org/10.1097/0000658-197302000-00017>.
- [37] Zhao S, Pinholt EM, Madsen JE, Donath K. Histological evaluation of different biodegradable and non-biodegradable membranes implanted subcutaneously in rats. *Journal of Cranio-Maxillo-Facial Surgery: Official Publication of the European Association for Cranio-Maxillo-Facial Surgery*. 2000; 28: 116–122. <https://doi.org/10.1054/jcms.2000.0127>.
- [38] Muire PJ, Mangum LH, Wenke JC. Time Course of Immune Response and Immunomodulation During Normal and Delayed Healing of Musculoskeletal Wounds. *Frontiers in Immunology*. 2020; 11: 1056. <https://doi.org/10.3389/fimmu.2020.01056>.
- [39] Dewey MJ, Harley BAC. Biomaterial design strategies to address obstacles in craniomaxillofacial bone repair. *RSC Advances*. 2021; 11: 17809–17827. <https://doi.org/10.1039/D1RA02557K>.
- [40] Van Leeuwen AC, Van Kooten TG, Grijpma DW, Bos RR. *In vivo* behaviour of a biodegradable poly(trimethylene carbonate) barrier membrane: a histological study in rats. *Journal of Materials Science. Materials in Medicine*. 2012; 23: 1951–1959. <https://doi.org/10.1007/s10856-012-4663-x>.
- [41] Jansen JA, de Ruijter JE, Janssen PT, Paquay YG. Histological evaluation of a biodegradable Polyactive/hydroxyapatite membrane. *Biomaterials*. 1995; 16: 819–827. [https://doi.org/10.1016/0142-9612\(95\)94142-8](https://doi.org/10.1016/0142-9612(95)94142-8).
- [42] Chia-Lai PJ, Orłowska A, Al-Maawi S, Dias A, Zhang Y, Wang X, *et al.* Sugar-based collagen membrane cross-linking increases barrier capacity of membranes. *Clinical Oral Investigations*. 2018; 22: 1851–1863. <https://doi.org/10.1007/s00784-017-2281-1>.
- [43] Gielkens PF, Schortinghuis J, de Jong JR, Raghoobar GM, Stegenga B, Bos RR. Vivosorb, Bio-Gide, and Gore-Tex as barrier membranes in rat mandibular defects: an evaluation by microradiography and micro-CT. *Clinical Oral Implants Research*. 2008; 19: 516–521. <https://doi.org/10.1111/j.1600-0501.2007.01511.x>.
- [44] van Erk M, Lomme RMLM, Roozen EA, van Oirschot BAJA, van Goor H. A novel *ex vivo* perfusion-based mandibular pig model for dental product testing and training. *BMC Oral Health*. 2023; 23: 122. <https://doi.org/10.1186/s12903-023-02794-6>.
- [45] Dorr DN, Frazier SD, Hess KM, Traeger LS, Srubar III WV. Bond Strength of Biodegradable Gelatin-Based Wood Adhesives. *Journal of Renewable Materials*. 2015; 3: 195–204. <https://doi.org/10.7569/jrm.2015.634108>.
- [46] Link DP, van den Dolder J, Jurgens WJ, Wolke JG, Jansen JA. Mechanical evaluation of implanted calcium phosphate cement incorporated with PLGA microparticles. *Biomaterials*. 2006; 27: 4941–4947. <https://doi.org/10.1016/j.biomaterials.2006.05.022>.
- [47] Ma X, Xu Z, Ding S, Yi G, Wang Q. Alendronate promotes osteoblast differentiation and bone formation in ovariectomy-induced osteoporosis through interferon- β /signal transducer and activator of transcription 1 pathway. *Experimental and Therapeutic Medicine*. 2018; 15: 182–190. <https://doi.org/10.3892/etm.2017.5381>.
- [48] Sharpe M, Noble S, Spencer CM. Alendronate: an update of its use in osteoporosis. *Drugs*. 2001; 61: 999–1039. <https://doi.org/10.2165/>

00003495-200161070-00010.

- [49] Rothamel D, Schwarz F, Fienitz T, Smeets R, Dreiseidler T, Ritter L, *et al.* Biocompatibility and biodegradation of a native porcine pericardium membrane: results of *in vitro* and *in vivo* examinations. The International Journal of Oral & Maxillofacial Implants. 2012; 27: 146–154.
- [50] Radenković M, Alkildani S, Stoewe I, Bielenstein J, Sundag B, Bellmann O, *et al.* Comparative *In Vivo* Analysis of the Integration Behavior and Immune Response of Collagen-Based Dental Barrier Membranes for Guided Bone Regeneration (GBR). Membranes. 2021; 11: 712. <https://doi.org/10.3390/membranes11090712>.
- [51] Wheat JC, Wolf JS Jr. Advances in bioadhesives, tissue sealants, and hemostatic agents. The Urologic Clinics of North America. 2009; 36: 265–275, x. <https://doi.org/10.1016/j.ucl.2009.02.002>.
- [52] Solomon SM, Sufaru IG, Teslaru S, Ghiciuc CM, Stafie CS. Finding the Perfect Membrane: Current Knowledge on Barrier Membranes in Regenerative Procedures: A Descriptive Review. Applied Sciences. 2022; 12: 1042. <https://doi.org/10.3390/app12031042>.
- [53] Wancket LM. Animal Models for Evaluation of Bone Implants and Devices: Comparative Bone Structure and Common Model Uses. Veterinary Pathology. 2015; 52: 842–850. <https://doi.org/10.1177/0300985815593124>.
- [54] Vajgel A, Mardas N, Farias BC, Petrie A, Cimões R, Donos N. A systematic review on the critical size defect model. Clinical Oral Implants Research. 2014; 25: 879–893. <https://doi.org/10.1111/clr.12194>.
- [55] Van Erk M, Van Luijk J, Yang F, Leeuwenburgh SCG, Sánchez-Fernández MJ, Hermans E, *et al.* A systematic review and meta-analyses on animal models used in bone adhesive research. Journal of Orthopaedic Research: Official Publication of the Orthopaedic Research Society. 2022; 40: 624–633. <https://doi.org/10.1002/JOR.25057>.
- [56] Alqahtani AM. Guided Tissue and Bone Regeneration Membranes: A Review of Biomaterials and Techniques for Periodontal Treatments. Polymers. 2023; 15: 3355. <https://doi.org/10.3390/polym15163355>.
- [57] Açıl Y, Zhang X, Nitsche T, Möller B, Gassling V, Wiltfang J, *et al.* Effects of different scaffolds on rat adipose tissue derived stroma cells. Journal of Cranio-Maxillo-Facial Surgery: Official Publication of the European Association for Cranio-Maxillo-Facial Surgery. 2014; 42: 825–834. <https://doi.org/10.1016/j.jcms.2013.11.020>.
- [58] Li J, Yan JF, Wan QQ, Shen MJ, Ma YX, Gu JT, *et al.* Matrix stiffening by self-mineralizable guided bone regeneration. Acta Biomaterialia. 2021; 125: 112–125. <https://doi.org/10.1016/j.actbio.2021.02.012>.
- [59] Song JM, Shin SH, Kim YD, Lee JY, Baek YJ, Yoon SY, *et al.* Comparative study of chitosan/fibroin-hydroxyapatite and collagen membranes for guided bone regeneration in rat calvarial defects: micro-computed tomography analysis. International Journal of Oral Science. 2014; 6: 87–93. <https://doi.org/10.1038/ijos.2014.16>.
- [60] Amoian B, Moudi E, Majidi MS, Ali Tabatabaei SM. A histologic, histomorphometric, and radiographic comparison between two complexes of CenoBoen/CenoMembrane and Bio-Oss/Bio-Gide in lateral ridge augmentation: A clinical trial. Dental Research Journal. 2016; 13: 446–453. <https://pmc.ncbi.nlm.nih.gov/articles/PMC5091004/>.
- [61] Cardaropoli D, Tamagnone L, Roffredo A, Gaveglione L, Cardaropoli G. Socket preservation using bovine bone mineral and collagen membrane: a randomized controlled clinical trial with histologic analysis. The International Journal of Periodontics & Restorative Dentistry. 2012; 32: 421–430.
- [62] Palachur D, Prabhakara Rao KV, Murthy KR, Kishore DT, Reddy MN, Bhupathi A. A comparative evaluation of bovine-derived xenograft (Bio-Oss Collagen) and type I collagen membrane (Bio-Gide) with bovine-derived xenograft (Bio-Oss Collagen) and fibrin fibronectin sealing system (TISSEEL) in the treatment of intra-bony defects: A clinico-radiographic study. Journal of Indian Society of Periodontology. 2014; 18: 336–343. <https://doi.org/10.4103/0972-124X.134572>.
- [63] Schlegel AK, Möhler H, Busch F, Mehl A. Preclinical and clinical studies of a collagen membrane (Bio-Gide). Biomaterials. 1997; 18: 535–538. [https://doi.org/10.1016/s0142-9612\(96\)00175-5](https://doi.org/10.1016/s0142-9612(96)00175-5).
- [64] Russell WMS. The Three Rs: past, present and future. Animal Welfare. 2005; 14: 279–286. <https://doi.org/10.1017/s0962728600029596>.
- [65] Meyerholz DK, Beck AP. Principles and approaches for reproducible scoring of tissue stains in research. Laboratory Investigation; a Journal of Technical Methods and Pathology. 2018; 98: 844–855. <https://doi.org/10.1038/s41374-018-0057-0>.
- [66] Holland T. The comparative power of the discriminant methods used in toxicological pathology. Toxicologic Pathology. 2005; 33: 490–494. <https://doi.org/10.1080/01926230590965382>.
- [67] Shackelford C, Long G, Wolf J, Okerberg C, Herbert R. Qualitative and quantitative analysis of nonneoplastic lesions in toxicology studies. Toxicologic Pathology. 2002; 30: 93–96. <https://doi.org/10.1080/01926230252824761>.
- [68] Mezei T, Kolcsár M, Joó A, Gurzu S. Image Analysis in Histopathology and Cytopathology: From Early Days to Current Perspectives. Journal of Imaging. 2024; 10: 252. <https://doi.org/10.3390/jimaging10100252>.
- [69] Mndlovu H, Kumar P, du Toit LC, Choonara YE. A review of biomaterial degradation assessment approaches employed in the biomedical field. npj Materials Degradation. 2024; 8: 66. <https://doi.org/10.1038/s41529-024-00487-1>.
- [70] Chen J, Lan Y, He Y, He C, Xu F, Zhang Y, *et al.* 99Tc-MDP-induced human osteoblast proliferation, differentiation and expression of osteoprotegerin. Molecular Medicine Reports. 2017; 16: 1801–1809. <https://doi.org/10.3892/mmr.2017.6839>.

Editor's note: The Scientific Editor responsible for this paper was Fergal J. O'Brien.

Received: 22nd November 2024; **Accepted:** 8th January 2025; **Published:** 26th June 2025